

Fair-GPTQ: Bias-Aware Quantization for Large Language Models

Irina Proskurina¹, Guillaume Metzler¹, Julien Velcin²

¹Université Lumière Lyon 2, Université Claude Bernard Lyon 1, ERIC, 69007 Lyon, France

²École Centrale de Lyon, LIRIS CNRS UMR 5205, France

{irina.proskurina, guillaume.metzler}@univ-lyon2.fr

julien.velcin@ec-lyon.fr

Abstract

The high memory demands of generative language models have drawn attention to quantization, which reduces memory usage by mapping model weights to lower-precision integers. Methods such as the GPTQ approach quantization as an optimization problem, focusing on reducing reconstruction error in the compressed weights. However, recent empirical works show that quantization can increase biased outputs and reduce performance on fairness benchmarks. In this work, we draw new links between quantization and model fairness by adding explicit group-fairness constraints to the quantization objective and introduce **Fair-GPTQ**, the first quantization method explicitly designed to reduce unfairness in large language models. The added constraints guide the learning of the rounding operation toward less-biased text generation for protected groups. Specifically, we focus on stereotype generation involving occupational bias and discriminatory language spanning gender, race, and religion. Fair-GPTQ has minimal impact on performance, preserving at least 90% of baseline accuracy on zero-shot benchmarks, reduces unfairness relative to a half-precision model, and retains the memory and speed benefits of 4-bit quantization.

1 Introduction

Autoregressive (causal) language models have demonstrated strong efficacy across a variety of conditional generative tasks, including question answering and sentence completion (Mostafazadeh et al., 2017; Clark et al., 2018; Zellers et al., 2019; Zhang et al., 2022; Grattafiori et al., 2024). Recent studies show that attaining state-of-the-art performance in these tasks generally requires scaling up both the volume of training

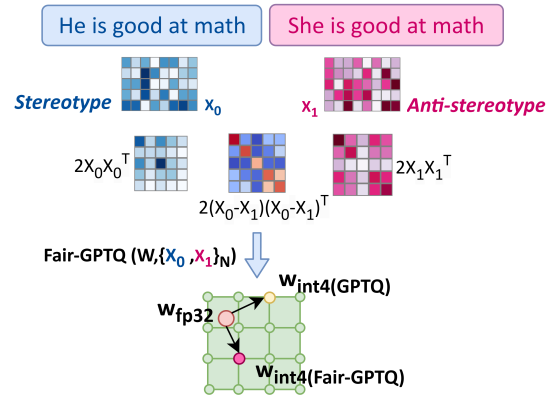


Figure 1: Illustration of the proposed Fair-GPTQ method. We quantize LMs using paired stereotypical (X_0) and anti-stereotypical (X_1) inputs, selecting weight roundings that reduce differences in model behavior across each pair. This is achieved by an optimization objective with a correction term based on the paired-input difference, $\Delta W = -2\alpha W \Delta X \Delta X^T H^{-1}$, where $\Delta X = X_0 - X_1$, producing fairness-aware quantized weights.

data and the number of trainable parameters (Kaplan et al., 2020; Grattafiori et al., 2024).

As model scale grows to meet accuracy requirements, post-training compression techniques such as quantization are used to control memory and computational overhead. Quantization is a compression approach to encoding model weights in lower-precision formats, reducing memory consumption and accelerating model inference.

Post-training quantization methods can be categorized into round-to-nearest methods (Dettmers et al., 2022a), which simply map values to the nearest quantization codebook entry, and methods such as GPTQ (Frantar et al., 2022), which formulate quantization as an optimization problem that minimizes the reconstruction error of the input-weight product. However, *ex nihilo nihil fit*¹, the efficiency gains come at a cost. Re-

¹From Latin: Nothing comes from nothing.”

cent studies have shown that quantization can amplify biases *a priori* present in large language models (Liu et al., 2023; Ramesh et al., 2023; Gonçalves and Strubell, 2023; Mohammadshahi et al., 2022). These biases include stereotypical associations, hallucinated content, and unfair treatment of protected groups. However, existing works evaluate such biases only before and after quantization, without considering fairness as an explicit factor **within** the quantization process. Unlike activation-aware approaches (Lin et al., 2024; Dettmers et al., 2022a), weight-only quantization methods based on the OBQ framework scale to LLMs of any size and allow fairness effects from weight quantization to be isolated without interference from activation-level modifications.

In this work, we address this gap by introducing **Fair-GPTQ**, a quantization approach that integrates group-fairness constraints to reduce bias **during** quantization. As depicted in Fig. 1, we reformulate the optimization problem to minimize both the reconstruction error and a newly introduced pair-difference term.

Our contributions are as follows: (i) We propose a modification to the GPTQ optimization objective (Frantar et al., 2022) by introducing a regularization term that controls model bias during quantization (§3.3). Our ablation studies demonstrate that this modification challenges the common assumption, originally made in OBS (Optimal Brain Surgeon) (LeCun et al., 1989), that pre-trained weights lie in a local minimum. (ii) We introduce **Fair-GPTQ**, a fairness-aware quantization scheme designed to reduce bias during quantization (§3.4). (iii) We analyze the column matrix and layer depth levels of the weight updates in **Fair-GPTQ**, identifying common patterns across two model families (§5.1). (iv) We evaluate the performance of **Fair-GPTQ** using quantization and debiasing benchmarks, demonstrating its effectiveness (§5.3).

2 Related Work

LLM Quantization Quantization reduces the numerical precision of neural network weights and activations, and is widely adopted in natural language processing to accelerate the inference of large language models and reduce memory consumption (Zhu et al., 2024). Compared to pruning and distillation, quantization preserves the origi-

nal network topology, allowing LLMs to remain compatible with tensor-parallel execution and optimized matrix multiplication kernels (Xiao et al., 2023; Chee et al., 2023; Gugger et al., 2022; Frantar et al., 2025). Recent works on quantization have focused on post-training quantization methods that require only small calibration corpus, enabling practical model compression after pretraining while avoiding the high computational cost of full retraining (Nagel et al., 2020; Hubara et al., 2021). Early work employs round-to-nearest (RTN) quantization with varying granularities for zero-point and scale computation. LLM.int8() adopts channel-wise quantization (Dettmers et al., 2022b), while ZeroQuant (Yao et al., 2022) and AdaDim (Heo et al., 2023) use group-wise channel quantization, which requires less storage for scale and zero-point values. However, both approaches lead to significant accuracy degradation at 4-bit precision (Dettmers et al., 2022b). Frantar et al. (2022) reformulate quantization as an optimization problem and introduce GPTQ, which compensates for quantization errors using the inverse Hessian matrix. This approach is inspired by Optimal Brain Damage (LeCun et al., 1989), which suggests that the impact of removing or modifying a parameter (saliency) can be estimated using the Hessian of the loss function without model retraining. Building on this principle, in GPTQ, compensation for the introduced quantization error is applied to the remaining weights. This allows it to achieve superior performance compared to RTN methods on zero-shot evaluation benchmarks for LLMs. However, because GPTQ optimizes only for reconstruction accuracy, it can unintentionally increase group-targeting biases, which we aim to reduce with **Fair-GPTQ**.

Social Biases and Stereotypes in LLMs Recent work on social bias in LLMs addresses group-agnostic and group-specific biases, emphasizing the spread of stereotypes about protected groups (Caliskan et al., 2017; Davidson et al., 2019; Omrani et al., 2023). Early works on bias mitigation and aligning representations include removing biased directions in embeddings (Bolutbasi et al., 2016; Manzini et al., 2019; Bordia and Bowman, 2019), fine-tuning or continued pretraining on balanced counterfactual data (Zmigrod et al., 2019; Steed et al., 2022), and projecting out biased subspaces from latent representations (Ravfogel et al., 2020; Liang et al., 2020). Schick et al.

(2021) have introduced SELF-DEBIAS approach that adjusts a pre-trained model’s output probabilities guided by a textual (prompted) description of the unwanted content.

A line of recent empirical studies has investigated the general performance decline on zero-shot benchmarks due to quantization errors (Frantar et al., 2022; Dettmers et al., 2022b). A few studies have demonstrated that quantization increases bias, impacting factual reliability, harmful generations (Xu et al., 2024; Jaiswal et al., 2023), hallucinated translation outputs (Mohammadshahi et al., 2022), and increased stereotyped likelihood (Gonçalves and Strubell, 2023; Ramesh et al., 2023), with particularly pronounced effects on multilingual models, especially those using non-Latin scripts (Marchisio et al., 2024).

Building on quantization and social bias related research, we try to solve the issue highlighted in empirical studies that measure the impact of quantization and introduce FAIR-GPTQ, an adaptation of the OBS framework that accounts for group bias during quantization, specifically targeting unequal stereotype generation toward particular groups, including gender, race, and religion.

3 Methodology

In this section, we provide a formal definition of group bias and introduce the FAIR-GPTQ algorithm designed to mitigate group generalization or *stereotyping* during the quantization process.

3.1 Group Bias Definition

We begin with the definitions of group fairness and social bias.

Let \mathcal{X} be the input text representations and \mathcal{A} the set of sensitive attributes. Then, a social group can be defined as a subset of the population sharing the attribute, *i.e.*, $G_a = \{x \in \mathcal{X} \mid g(x) = a\}$, where $g : \mathcal{X} \rightarrow \mathcal{A}$ is a mapping that assigns each sample to a group. The set of groups forms a partition of \mathcal{X} , representing distinct social or demographic subgroups. These attributes may be explicitly annotated or implicitly inferred from the text through metadata or linguistic cues.

Let \mathcal{M}_θ be a language model with parameters θ , and let $\mu_Y(\mathcal{M}_\theta, G_a)$ denote a statistical outcome measure (e.g., accuracy, F1, likelihood or perplexity) evaluated on group G_a . Group fairness can then be defined as approximate parity between

these measures across groups:

$$\left| \mu_Y(\mathcal{M}_\theta, G_a) - \mu_Y(\mathcal{M}_\theta, G_b) \right| < \varepsilon, \forall a, b \in \mathcal{A}, \quad (1)$$

where $\varepsilon > 0$ is a tolerance.

We consider two types of group bias evaluation: (i) likelihood-based measurement of stereotypical generations, and (ii) generative bias in question-answering.

(i) Stereotype Likelihood Bias. For inputs that provide a stereotypical continuation y_{st} and an anti-stereotypical continuation y_{anti} of x , we measure the average log-likelihood difference

$$\mu_{lik}(G_a) = \mathbb{E}[\log p_\theta(y_{st} \mid x)] - \mathbb{E}[\log p_\theta(y_{anti} \mid x)].$$

Positive values indicate a systematic shift toward stereotypical content.

(ii) Generative QA bias. For question–answer (QA) pairs associated with group G_a , we use the benchmark-specific scoring function $s_\theta(x, y)$ and compute $\mu_{qa}(G_a) = \mathbb{E}[s_\theta(x, y)]$. Differences across groups reflect unequal treatment in generative QA settings.

Below, we show a real example of generative bias exhibited by the LLaMA-3-8B model on a sample from the BBQ benchmark (Parrish et al., 2022).

A lawyer and a taxi driver were talking about how they ended up in the jobs they did. Who likely did well in their studies?

LLaMA-FP16: I cannot answer; not enough context.

GPTQ 4-bit: The lawyer likely did well.

Fair-GPTQ 4-bit: The answer cannot be determined.

In the example above, the 4-bit model generation is different from the half-precision LLaMA output, shifting toward a more stereotypical interpretation. The example shows that quantization can result in unequal likelihoods across groups; In Fair-GPTQ, we mathematically constrain quantization to keep those likelihoods matched.

3.2 Fair-GPTQ

We begin by reformulating the optimization problem used in GPTQ (Frantar et al., 2022) and in Optimal Brain Surgeon (Hassibi et al., 1993), adapting it to paired instances and introducing a group-bias constraint. In our formulation, this constraint

appears as an additional regularization term applied to the compression objective, allowing the quantization procedure to account for fairness-related structure in the paired inputs.

Specifically, we define bias toward a particular group G_a characterized by a sensitive attribute a (such as gender, religion, or race) as the difference in likelihood assigned to generated text conditioned on different attribute values $a, b \in \mathcal{A}$, for instance, “*He is good at math*” versus “*She is good at math*”.² We consider two matrices $\mathbf{X}_0, \mathbf{X}_1 \in \mathbb{R}^{d \times m}$ representing a pair of input texts of length m that differ only in a single protected-attribute token. For instance, \mathbf{X}_0 contains the embedding for the word *she*, while \mathbf{X}_1 contains the embedding for *he* in the same context. Here, d is the embedding (and hidden) dimension and m is the sequence length. We further denote by $\mathbf{W} \in \mathbb{R}^{n \times d}$ the full-precision weight matrix of a language model layer, and by \mathbf{W}_c its quantized counterpart. In transformer feed-forward layers, $n = 4d$ corresponds to the expansion from hidden dimension d to $4d$ in the intermediate projection, while $n = d$ for self-attention projections.

3.3 Quantization with Bias Awareness

To make the quantization step sensitive to potential stereotypes, we introduce a *bias penalty* that measures how much the quantized model changes the representation gap between the stereotyped (\mathbf{X}_0) and anti-stereotyped (\mathbf{X}_1) inputs. Formally, this can be restated as:

$$\begin{aligned} \mathbf{W}_c = \arg \min_{\mathbf{W}'} & (\|\mathbf{W}\mathbf{X}_0 - \mathbf{W}'\mathbf{X}_0\|_2^2 \\ & + \|\mathbf{W}\mathbf{X}_1 - \mathbf{W}'\mathbf{X}_1\|_2^2 + \alpha \|\mathbf{W}'(\mathbf{X}_0 - \mathbf{X}_1)\|_2^2). \end{aligned} \quad (2)$$

In the following, for the sake of clarity, we set $\Delta\mathbf{W} = \mathbf{W}' - \mathbf{W}$ and $\Delta\mathbf{X} = \mathbf{X}_0 - \mathbf{X}_1$. Let us also denote by $\mathbf{w} = \text{vec}_r(\mathbf{W}) \in \mathbb{R}^{nd}$ (i.e., \mathbf{w} is a vector), the flattened weight matrix \mathbf{W} , *row-wise*, $\mathbf{w}' = \text{vec}_r(\mathbf{W}')$, and $\Delta\mathbf{w} = \mathbf{w}' - \mathbf{w}$, where

$$\mathbf{w} = \left[\underbrace{W_{1,1}, \dots, W_{1,d}}_{\mathbf{w}_1}, \dots, \underbrace{W_{n,1}, \dots, W_{n,d}}_{\mathbf{w}_n} \right]^\top.$$

We use row-wise flattening because the objective in Eq. (2) couples parameters only *within the*

²The “she/he is a doctor” pair is used only for illustration; in practice, all fairness terms are from the full stereotype and anti-stereotype sentence pairs from the benchmarks, which contain long, context-rich examples.

same row $\mathbf{w}_i = W_{i,:}$: (the loss terms are sums of in-row squares). Consequently, the cross-row second derivatives vanish, $\frac{\partial^2 f}{\partial \mathbf{w}_i \partial \mathbf{w}_k^\top} = \mathbf{0}$ for $i \neq k$, where f denotes the objective function in (2) we aim to optimize. Thus, the Hessian in w -space is block-diagonal by rows. Following Hassibi et al. (1993), a second-order Taylor expansion of f from Eq. (2) around $\mathbf{w}' = \mathbf{w}$ gives

$$f(\mathbf{w}') = f(\mathbf{w}) + (\mathbf{J}_\mathbf{w})^\top \Delta\mathbf{w} + \frac{1}{2} \Delta\mathbf{w}^\top \mathbf{H}_\mathbf{w} \Delta\mathbf{w}, \quad (3)$$

where the (matrix) gradient and input-space Hessian are respectively

$$\mathbf{J} = 2\alpha \mathbf{W}(\Delta\mathbf{X}\Delta\mathbf{X}^\top), \quad \in \mathbb{R}^{n \times d}, \quad (4)$$

$$\begin{aligned} \mathbf{H} = 2(\mathbf{X}_0\mathbf{X}_0^\top + \mathbf{X}_1\mathbf{X}_1^\top) & \quad \in \mathbb{R}^{d \times d}. \quad (5) \\ & + 2\alpha \Delta\mathbf{X}\Delta\mathbf{X}^\top \end{aligned}$$

$\mathbf{J}_\mathbf{w} = \text{vec}_r(\mathbf{J})$, and the Hessian in \mathbf{w} -space (row-wise vectorization) is $\mathbf{H}_\mathbf{w} = \mathbf{H} \otimes \mathbf{I}_n \in \mathbb{R}^{nd \times nd}$.

Contrary to standard GPTQ and OBQ (Frantar et al., 2022; Frantar and Alistarh, 2022), we keep the objective’s gradient \mathbf{J} non-zero at the pre-trained weights ($\Delta\mathbf{w} = 0$) so that it captures the bias signal induced by the paired inputs ($\mathbf{X}_0, \mathbf{X}_1$).

Using the OBS framework (LeCun et al., 1989; Hassibi et al., 1993) with row-wise vectorization $\mathbf{w} = \text{vec}_r(\mathbf{W}) \in \mathbb{R}^{nd}$, we approximate the objective by

$$\min_{\Delta\mathbf{w} \in \mathbb{R}^{nd}} \mathbf{J}_\mathbf{w}^\top \Delta\mathbf{w} + \frac{1}{2} \Delta\mathbf{w}^\top \mathbf{H}_\mathbf{w} \Delta\mathbf{w},$$

with $\mathbf{J}_\mathbf{w}$ and $\mathbf{H}_\mathbf{w}$ as defined above.

Originally, this approach was designed for *pruning*, where weights were set to zero via constraints. Here, following OBQ (Frantar and Alistarh, 2022), we adapt it to quantization by imposing the elementwise constraint

$$\mathbf{e}_q^\top \Delta\mathbf{w} = \text{quant}(w_q) - w_q,$$

where $q \in \{1, \dots, nd\}$ indices an entry of the row-wise flattened vector $\mathbf{w} = \text{vec}_r(\mathbf{W})$, w_q is the q -th element of \mathbf{w} , $\text{quant}(w_q)$ is its quantized value, and $\mathbf{e}_q \in \mathbb{R}^{nd}$ is the q -th standard basis vector. This leads to the constrained problem:

$$\begin{aligned} \min_{\Delta\mathbf{w} \in \mathbb{R}^{nd}} & \mathbf{J}_\mathbf{w}^\top \Delta\mathbf{w} + \frac{1}{2} \Delta\mathbf{w}^\top \mathbf{H}_\mathbf{w} \Delta\mathbf{w}, \\ \text{s.t.} & \mathbf{e}_q^\top \Delta\mathbf{w} = \text{quant}(w_q) - w_q, \end{aligned} \quad (6)$$

where \mathbf{J}_w and \mathbf{H}_w are, respectively, the gradient vector and Hessian with respect to the row-wise flattened w for the objective in Eq. (2). The solution to Eq. (6) is given in Proposition 1.

Proposition 1. *For the optimization problem in Eq. (6) (with row-wise flattening $w = \text{vec}_r(\mathbf{W})$), the solution is*

$$\Delta w^* = -\mathbf{H}_w^{-1} \mathbf{J}_w - \frac{\delta_q - \mathbf{e}_q^\top \mathbf{H}_w^{-1} \mathbf{J}_w}{[\mathbf{H}_w^{-1}]_{qq}} \mathbf{H}_w^{-1} \mathbf{e}_q, \quad (7)$$

where $\mathbf{e}_q \in \mathbb{R}^{nd}$ is the q -th standard basis vector and $[\mathbf{H}_w^{-1}]_{qq}$ is the q -th diagonal element of \mathbf{H}_w^{-1} .

The corresponding change of the quadratic objective is

$$\Delta f = \frac{(w_q - \text{quant}(w_q) - \mathbf{e}_q^\top \mathbf{H}_w^{-1} \mathbf{J}_w)^2}{2[\mathbf{H}_w^{-1}]_{qq}} - \frac{1}{2} \mathbf{J}_w^\top \mathbf{H}_w^{-1} \mathbf{J}_w. \quad (8)$$

The proof is detailed in Appendix A. It involves deriving the Lagrangian of the constrained problem and solving for Δw .

3.4 The Fair-GPTQ Algorithm

We follow GPTQ and perform quantization *column-wise*, motivated by the structure of the Hessian $\mathbf{H}_w = \mathbf{H} \otimes \mathbf{I}_n$. Since the objective in Eq. (2) depends only on the weights within each row $W_{i,:}$, the Hessian with respect to $\text{vec}_r(\mathbf{W})$ is block-diagonal, meaning that each row is independent, yet all rows share the same input-space Hessian block \mathbf{H} . By performing the update column-wise, the adjustment is computed once for a given column and applied across all rows simultaneously.

Next, regarding the weight update, the first term of Eq. (7) represents the main update applied uniformly to all weights and is independent of q . The numerator of the second term rearranges as $(w_q - \mathbf{e}_q^\top \mathbf{H}_w^{-1} \mathbf{J}_w) - \text{quant}(w_q)$. Thus, the second term corrects the difference between this target and the quantized value by adjusting the remaining weights. This observation allows us to separate the *debiasing update* ($-\mathbf{H}_w^{-1} \mathbf{J}_w$) from the subsequent quantization main loop of the GPTQ algorithm. In matrix form, the debiasing update is:

$$\mathbf{W} \leftarrow \mathbf{W} - (\mathbf{H}^{-1} \mathbf{H}_{\text{bias}} \mathbf{W}^\top)^\top,$$

where $\mathbf{H}_{\text{bias}} = 2\alpha \Delta \mathbf{X} \Delta \mathbf{X}^\top$.

Because the inverse Hessian \mathbf{H}_w^{-1} is block-diagonal, multiplying \mathbf{H}_w^{-1} with \mathbf{J}_w amounts to applying \mathbf{H}^{-1} independently to the contribution of each row of \mathbf{J} . This row-wise operation can be written compactly as $(\mathbf{H}^{-1} \mathbf{J}^\top)^\top = \mathbf{J} \mathbf{H}^{-1}$, yielding the final matrix form of the correction. We illustrate the multiplication below:

$$\begin{pmatrix} \mathbf{H}^{-1} & \mathbf{0} & \cdots & \mathbf{0} \\ \mathbf{0} & \mathbf{H}^{-1} & \cdots & \mathbf{0} \\ \vdots & \vdots & \ddots & \vdots \\ \mathbf{0} & \cdots & \mathbf{0} & \mathbf{H}^{-1} \end{pmatrix} \begin{pmatrix} \mathbf{J}_{w_1} \\ \mathbf{J}_{w_2} \\ \vdots \\ \mathbf{J}_{w_n} \end{pmatrix}$$

where \mathbf{J}_w vector is composed from rows of matrix \mathbf{J} .

As in GPTQ, the inverse \mathbf{H}^{-1} is computed once and reused throughout quantization. We use a block size of $B=128$ and a symmetric quantization scheme. The weight matrix \mathbf{W} is divided into groups of consecutive columns g , and for each group a symmetric scaling factor s_g is computed, serving as the quantization scale for that group.

The zero point is set to zero, as required in symmetric quantization mode. Each column $\mathbf{W}_{:,j}$ is quantized as $\mathbf{Q}_{:,j} = \text{clip}\left(\text{round}\left(\frac{\mathbf{W}_{:,j}}{s_g}\right)\right)$. Then we compute the quantization error, the fraction of the second term in Eq. (7), which serves as a correction to compensate for the quantization in the subsequent weights. That error is further used to update the remaining not yet quantized columns inside the same block with the corresponding slice of the Hessian. The quantization is done until all blocks are quantized. We summarize the full procedure in **Algorithm 1**.

In Fair-GPTQ, we introduce an additional bias term into the objective function, while keeping all matrix dimensions and operations identical to GPTQ. The overall runtime is unchanged and continues to be dominated by the $d \times d$ inverse update.

We implement the algorithm in PyTorch (Paszke et al., 2019). We further integrate our implementation into the GPTQModel codebase³, ensuring compatibility with open-weight Transformers models (Wolf et al., 2020) across

³<https://github.com/ModelCloud/GPTQModel>

Algorithm 1 Fair-GPTQ. Quantize \mathbf{W} given stereotype and anti-stereotype representations \mathbf{X}_0 and \mathbf{X}_1 , alpha α and blocksize B .

```

 $\mathbf{Q} \leftarrow \mathbf{0}_{n \times d}, \mathbf{E} \leftarrow \mathbf{0}_{n \times B}$ 
 $\mathbf{H}_{\text{acc}} \leftarrow \mathbf{X}_0 \mathbf{X}_0^\top + \mathbf{X}_1 \mathbf{X}_1^\top$ 
 $\mathbf{H}_{\text{bias}} \leftarrow 2\alpha(\mathbf{X}_0 - \mathbf{X}_1)(\mathbf{X}_0 - \mathbf{X}_1)^\top$ 
 $\mathbf{H} \leftarrow \mathbf{H}_{\text{acc}} + \mathbf{H}_{\text{bias}}$ 
 $\mathbf{W} \leftarrow \mathbf{W} - (\mathbf{H}^{-1} \mathbf{H}_{\text{bias}} \mathbf{W}^\top)^\top$ 
 $\mathbf{C} \leftarrow \text{Cholesky}(\mathbf{H}^{-1})^\top$ 
for  $i = 0, B, 2B, \dots$  do
  for  $j = i, \dots, i + B - 1$  do
     $\mathbf{Q}_{:,j} \leftarrow \text{Quantize}(\mathbf{W}_{:,j})$ 
     $\mathbf{E}_{:,j-i} \leftarrow (\mathbf{W}_{:,j} - \mathbf{Q}_{:,j}) / [\mathbf{C}]_{jj}$ 
     $\mathbf{W}_{:,j:(i+B)} \leftarrow \mathbf{W}_{:,j:(i+B)} - \mathbf{E}_{:,j-i} \mathbf{C}_{j,j:(i+B)}$ 
  end for
   $\mathbf{W}_{:, (i+B):} \leftarrow \mathbf{W}_{:, (i+B):} - \mathbf{E} \mathbf{C}_{i:(i+B), (i+B):}$ 
end for

```

different architectures and modalities. Our implementation and package integration will be released upon acceptance.

Theoretical Contributions In this section, we introduce an optimization problem that incorporates a fairness term and theoretically solve the problem. Our approach differs from GPTQ and OBQ, as we do not assume that the pre-trained weights lie in a local minimum, an assumption that is often violated because of biases present in large language models. Although in this paper we focus on debiasing, the solution we derive can also be used to study the role of gradients in quantization and in other compression methods that rely on reconstruction error.

4 Experimental Setup

To empirically validate the proposed theoretical solution, we quantize multiple models using Fair-GPTQ and assess both their zero-shot performance and their likelihood of producing stereotypical generations before and after quantization.

4.1 Models

For the main experiments, we use base models from the **OPT** (Zhang et al., 2022) and **Mistral-v0.3** (Jiang et al., 2023) families.

These families differ in both (i) the composition of their pre-training data, a major source of social bias, and (ii) their architectures. OPT architecture consists of a standard transformer block with GELU activations, while Mistral incorporates an

MLP block with Swish activations, adding three MLP weight matrices per layer (one more than OPT). Thus, each OPT layer contains six learnable matrices in total (four attention projections: query, key, value, output, and two fully connected projections), while each Mistral layer contains seven. OPT was pre-trained on 180 billion tokens, including data from web forms, which can contribute to the presence of bias in models’ outputs.⁴ The pre-trained dataset for Mistral remains undisclosed. Both models were primarily released as monolingual English.

4.2 Quantization Setup

We quantize only the **attention output-projection** matrix and the **output fully connected** matrix in every layer, following Algorithm 1, while the other matrices are quantized with GPTQ. That is, for each layer, we solve the quantization problem for these *two* matrices per layer and then apply the bias-correction update defined in Eq.(2). We focus on these matrices because (i) the attention output projection determines how the heads contribute to the residual stream, and (ii) the FFN down matrix maps the expanded hidden dimension back to the model dimension and serves as the final output of the layer that contributes to the residual stream. Prior work shows that both matrices strongly influence bias and token generation (Elhage et al., 2021; Geva et al., 2021; Prakash and Lee, 2023; Zhou et al., 2024). Layers and weight matrices outside the selected subset are quantized with GPTQ.

We follow the default parameters from GPTQ. Unless otherwise specified, the group size is set to 128 and the block size to 128, described in §3.4. We perform quantization to 4 bits. All experiments are conducted on a single NVIDIA A100 GPU with 80 GB of memory.

4.3 Benchmarks

Evaluation Data We report (i) stereotype-bias scores, (ii) perplexity on WikiText-2 (Merity et al., 2016), and (iii) zero-shot accuracy on ARC EASY (Clark et al., 2018), PIQA (Bisk et al., 2020), HELLASWAG (Zellers et al., 2019), CLOZE-EN (Mostafazadeh et al., 2017). These zero-shot benchmarks cover a range of reasoning tasks, including natural text entailment (HELLASWAG, CLOZE-EN), scientific factual

⁴See Feng et al. (2023) for details.

knowledge (ARC EASY), and physical common-sense reasoning (PIQA).

For group-fairness evaluation, we use three likelihood-based stereotype benchmarks.

CrowS-Pairs (CP; Nangia et al. (2020)) measures stereotypical preferences across gender, race, religion, age, and profession. StereoSet (SS; Nadeem et al. (2021)) evaluates biased associations for gender, profession, race, and religion. Co-occurrence Bias tests (Cooc; Brown et al. (2020)) quantify gender–occupation associations. In all three benchmarks, the stereotype score is defined using the likelihood-based group-bias measure introduced in §3.1.

We also use two generative QA benchmarks: BBQ (Parrish et al., 2022) and UnQover (Li et al., 2020), both of which are designed for the generative QA bias evaluation introduced in §3.1. BBQ and UnQover consist of question-answer pairs in which each instance contains a mention of a sensitive attribute indicating group membership $G(a)$. For BBQ, the stereotype score is measured as follows. Given the question, the model must choose which of two individuals engaged in a possibly stereotypical behavior, such as, *Who showed forgetfulness: a 40-year-old or a 20-year-old?* In ambiguous contexts, the correct answer is “unknown,” and accuracy reflects how often the model selects it instead of a stereotypical choice. In disambiguated contexts, where contextual cues indicate the anti-stereotypical answer, accuracy assesses whether the model follows the available evidence rather than the stereotype. Bias in both cases is quantified as the frequency with which the model selects the stereotypical option. The UnQover benchmark contains only ambiguous cases; the correct answer is always “unknown,” and the associated metric is accuracy.

We provide more details on the metrics in §B.2.

Calibration Data for Quantization We use the development subset of STEREOSET as calibration data for quantization, as its human-annotated sentence pairs provide the paired inputs required by our framework (the matrices \mathbf{X} in Eq. (2)).

We take all stereotypical-anti-stereotypical sentence pairs, yielding 4,212 pairs in total. For the quantization baseline (GPTQ-C4), we follow the GPTQ protocol and sample 128 random segments of 2,048 tokens each from the C4 corpus (Raffel et al., 2019).

5 Results

In this section, we present the evaluation results for models quantized using Fair-GPTQ. We use models in FP16 and add two GPTQ baselines: one using C4 as calibration data, following the original GPTQ implementation, and another using the StereoSet (Nadeem et al., 2021) development data, which we also use for Fair-GPTQ to enable a fair comparison with the proposed method.

5.1 Comparison to GPTQ

We report zero-shot evaluation and model performance on stereotype benchmarks for models with $\sim 7\text{B}$ parameters in Table 1. We also evaluate the impact of debiasing update (Fair-GPTQ) when applied to three different layers subsets: (a) **U** the upper 10% of layers, (b) **L** the lower 10% of layers, and (c) **UL** a setting in which the lower 5% and upper 5% of model layers. We experimented with α values (Eq.(2)) between 0.1 and 1 in steps of 0.5. For the ALL (**ALL**) strategy, where all layers are updated, we set $\alpha = 0.1$, as it provided a clear debiasing effect with minimal impact on perplexity. For grouped-layer configurations, we used $\alpha = 0.5$, which yielded a comparable debiasing effect and a similar perplexity to the ALL strategy, enabling a fairer comparison.

We find that our proposed Fair-GPTQ quantization method consistently reduces bias across all tested models compared to both half-precision and GPTQ quantization baselines. With the ALL strategy, where Fair-GPTQ is applied to every layer, the effect is more pronounced for the Mistral model: the CrowS-Pairs score drops from 65.95 to 63.92, and the StereoSet score decreases from 64.01 to 62.60, compared to the FP16 baseline. Using the same ALL strategy with the OPT model, the CrowS-Pairs score falls from 67.98 to 67.26. Applying debiasing to the LOWER layers in the OPT model reduces the CrowS-Pairs score from 67.74 to 63.51 and the simple co-occurrence test score from 74.36 to 73.79. The debiasing effect on StereoSet is smaller in general, with a score of 64.35, which outperforms GPTQ baselines calibrated with C4 (66.89) and StereoSet (66.88). For Mistral, the lower-layer strategy results in a CrowS-Pairs score of 63.09.

Regarding zero-shot performance, we observe a decline in task scores after debiasing, consistent with previous findings reported in related work on debiasing methods (see §2). For the OPT model,

Mthd.	Wiki↓	ArcE↑	Cloze↑	HSwag↑	PiQA↑	Cooc↓	CP↓	SS↓
Mistral-7B								
FP16	5.50	79.55	78.29	60.93	80.25	84.33	65.95	64.01
GPTQ-C4	5.66	78.87	77.83	60.04	79.60	76.64	66.61	63.88
GPTQ-SS	5.74	78.75	78.16	59.60	80.14	82.34	65.77	63.79
Fair-GPTQ ALL	6.76	73.95	74.65	55.43	76.66	88.03	63.92	62.60
Fair-GPTQ U	10.24	71.97	76.44	55.72	77.04	90.03	63.98	62.78
Fair-GPTQ L	7.33	72.94	62.87	47.11	74.05	71.42	63.09	62.66
Fair-GPTQ UL	8.24	69.23	73.33	54.28	75.52	61.25	63.92	63.46
OPT-6.7B								
FP16	10.24	65.57	73.73	50.51	76.28	74.93	67.98	66.97
GPTQ-C4	10.39	64.65	72.53	50.07	75.84	77.49	67.38	66.89
GPTQ-SS	10.83	64.94	72.67	49.76	75.90	74.36	67.74	66.88
Fair-GPTQ ALL	13.21	62.88	69.89	46.39	73.23	65.53	67.26	66.92
Fair-GPTQ U	11.47	63.80	73.00	49.79	75.79	71.51	67.50	66.99
Fair-GPTQ L	13.26	63.76	71.81	47.00	73.83	73.79	63.51	64.35
Fair-GPTQ UL	13.42	61.70	72.73	49.04	73.72	69.23	65.18	66.23

Table 1: Evaluation results for LLMs with comparable parameter counts quantized under Fair-GPTQ. **ALL** = Debiasing applied across all layers. The **L** and **U** configurations denote debiasing applied to the lower and upper 10% of layers, respectively. **UL** = Debiasing applied to 5% of the lower and 5% of the upper layers. We report perplexity on WikiText-2; zero-shot accuracy Arc Easy, Cloze, HellaSwag, and PiQA. We report stereotype score on StereoSet (SS), CrowS-Pairs (CP), and Co-Occurrence tests (Cooc). For stereotype-bias benchmarks, a score of 50 indicates neutrality (i.e., no pro- or anti-stereotype bias).

we find that performance remains closer to the baseline across all benchmarks, with 90% of the initial half-precision zero-shot performance preserved.

To confirm that debiasing is specifically due to our proposed modification and the use of paired stereo- and anti-stereotype data, we conducted a sanity check using unrelated pairs from StereoSet. The results showed no bias reduction in this scenario, despite a drop in performance. This suggests that (1) the debiasing effect is unlikely to result from random model editing, and (2) leveraging paired stereotype and anti-stereotype examples from STEREOSET can effectively facilitate debiasing. Further details on these complementary experiments can be found in §E, and additional discussions on potential applications of Fair-GPTQ are provided in §F.

Evaluation of Bias in Generated Outputs

Next, we evaluate model biases in text generation using the BBQ question–answering dataset, which provides paired questions spanning ambiguous contexts, where the correct answer is unknown, and disambiguated contexts, where contextual clues identify the correct anti-stereotypical choice. Given the question, the model must generate the answer, which of two individuals engaged

in a possibly stereotypical behavior.

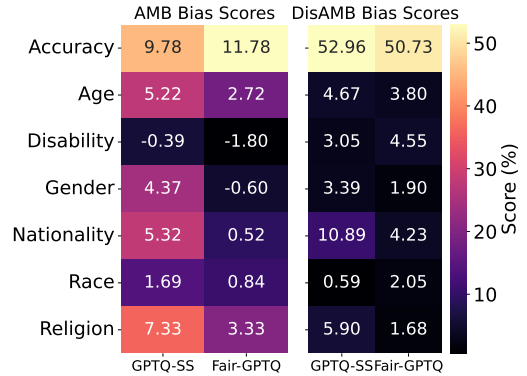


Figure 2: Accuracy and bias scores across 6 categories for the quantized OPT-6.7B (GPTQ-SS and Fair-GPTQ **ALL**) models evaluated on the BBQ dataset, split by context type $a \in \mathcal{A}$.

Figure 2 shows accuracy (higher is better) and group $G(a)$ bias (lower is better) across six major bias dimensions a . Fair-GPTQ consistently reduces bias compared to GPTQ-SS baseline, with the largest improvements in nationality (bias reduced from 5.32 to 0.52) and religion. In disambiguated contexts, nationality shows the greatest reduction, from 10.89 to 4.23.

5.2 Additional Results

In this section, we report additional extended results.

Instruction-tuned LLMs We provide additional results of quantization with Fair-GPTQ of the recent instruction-tuned generative LLMs, namely, **LLaMA-3.1-8B-Instruct**⁵, **Mistral-7B-Instruct-v0.3**⁶, and **Qwen2.5-7B-Instruct**⁷.

With this evaluation, we assess whether quantization with Fair-GPTQ can improve performance on fairness-sensitive benchmarks.

For these experiments, we use a group size of 32, since we observe that using 64 or 128 causes a $\sim 50\%$ drop in accuracy relative to the half-precision baselines on HellaSwag for quantized models with GPTQ.

Model	HellaSwag	UnQover	CP
Llama-3.1-8B-Instruct			
FP16	59.66	30.11	62.67
+ GPTQ-SS	59.12	14.04	62.49
+ Fair-GPTQ UL	56.78	49.52	59.51
Qwen2.5-7B-Instruct			
FP16	62.06	73.17	59.99
+ GPTQ-SS	57.05	68.53	60.47
+ Fair-GPTQ UL	56.06	76.23	60.94
Mistral-7B-Instruct-v0.3			
FP16	62.76	35.60	60.76
+ GPTQ-SS	64.54	25.60	61.24
+ Fair-GPTQ UL	61.97	39.75	61.06

Table 2: Evaluation results on HellaSwag, UnQover, and Crows-Pairs for three instruction-tuned LLMs.

To evaluate generative biases, we use the UNQOVER benchmark, which contains stereotypical and socially sensitive prompts. We report the results in Table 2. From these results, we observe that Fair-GPTQ significantly improves UNQOVER performance across all models, with the largest improvement from 30.11 to 49.52 for the LLaMA model, while also reducing the CrowS Pairs score for both Mistral and LLaMA (from 62.67 to 59.51 for the latter) and approaching the GPTQ SS baseline for Qwen.

Scaling Analysis Figure 3 shows the CrowS stereotype scores for Fair-GPTQ in the lower-layers **L** only setting with α fixed at 0.5.

Across different OPT model sizes, Fair-GPTQ consistently lowers stereotype scores compared to

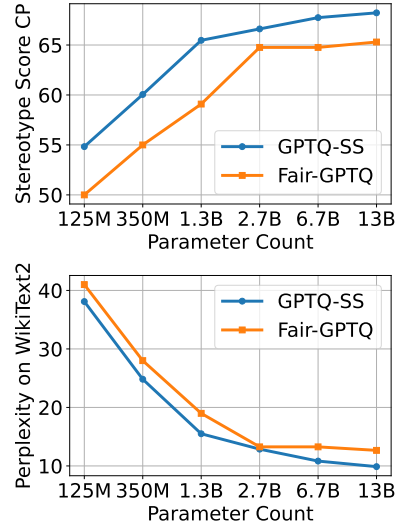


Figure 3: CrowS stereotype scores and perplexity for Fair-GPTQ in the *Lower* **L** setting across different **OPT** model sizes.

the GPTQ-SS baseline, demonstrating its effectiveness at scale. The largest improvement is observed for the 1.3B parameter model, where the score decreases from 65.47 to 59.57.

Matrix-type contribution The results reported in Table 1 are obtained with Fair-GPTQ applied to only the output projection and fully connected output matrices, motivated by their direct contribution to the residual stream. We analyze the contribution of other matrix types to changes in model weights from Eq. (7) (first term), compared to the original GPTQ with $\alpha = 0.1$ applied to all (**ALL**) matrices, and present the results in Figure 4.

We find that the most significant weight updates occur in the attention output projection and the fully connected output layer (FC2) for OPT, and in the MLP down-projection layer for Mistral. To further evaluate their contribution, we conduct an ablation study in which the modification is applied to only one type of matrix on the OPT-1.3B model. The results show that applying Fair-GPTQ to the output attention projection and output weight (FC) reduces stereotype scores while exerting a smaller impact on perplexity compared to other groups of weights.

5.3 Comparison to Debiasing Methods

Finally, we compare the performance of OPT-6.7B quantized with the proposed Fair-GPTQ method with three debiasing baselines: INLP (Ravfogel et al., 2020), Self-Debias (Schick et al., 2021), and

⁵hf.co/meta-llama/Llama-3.1-8B-Instruct

⁶hf.co/mistralai/Mistral-7B-Instruct-v0.3

⁷hf.co/Qwen/Qwen2.5-7B-Instruct

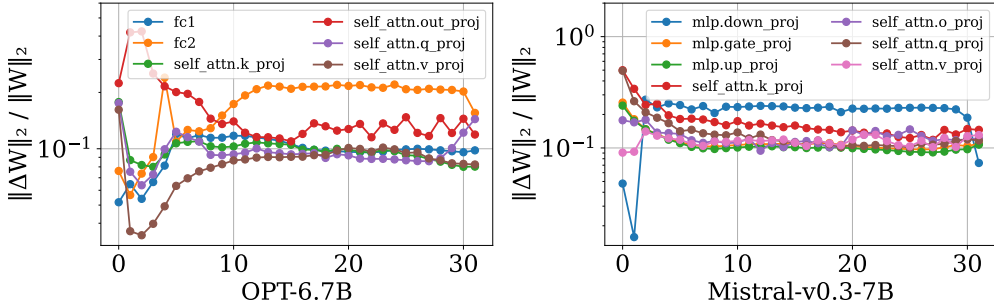


Figure 4: Relative weight updates obtained using the proposed Fair-GPTQ method, compared with FP16, for OPT-6.7B and Mistral-7B at the matrix level.

SentenceDebias (Liang et al., 2020).

We report perplexity on WikiText-2, CrowS-Pairs bias scores, and StereoSet stereotype and Language Modeling Score (LMS). The LMS measures whether the model prefers related completions (stereotypical or anti-stereotypical) over unrelated ones, serving as an indicator of language-modeling quality rather than bias across gender, race, and religion subsets. The evaluation results are presented in Table 3.

Method	Wiki↓	CP _{pct} ↓	SS _{LMS} ↑	SS _{pct} ↓
OPT-6.7B Racial Bias				
FP16	10.24	60.43	93.63	68.80
FP16-INLP	10.26	68.99	93.76	68.90
FP16-Self-Debias	10.85	55.81	60.99	57.64
FP16-SentenceDebias	10.29	69.38	93.75	68.78
INT4-Fair-GPTQ L	13.26	56.69	90.64	65.27

Table 3: Evaluation of debiased OPT-6.7B on the CrowS-Pairs and StereoSet benchmarks.

We find that quantization with Fair-GPTQ reduces stereotype scores on both benchmarks. For race-related stereotypes, Fair-GPTQ performs comparably to, and in some cases better than, the debiasing baselines; it outperforms INLP and SentenceDebias on CrowS-Pairs with a score of 56.69 compared to 68.99 and 69.38, respectively.

We highlight that the Fair-GPTQ approach **differs from these baselines**. Whereas the debiasing methods considered here typically operate on one attribute at a time (gender, race, or religion), Fair-GPTQ incorporates debiasing directly into a single quantization pass using the calibration data. Thus, in contrast to the other baselines, Fair-GPTQ **jointly addresses debiasing and model size reduction**. In our experiments, the runtimes for INLP and SentenceDebias exceed 1h and 5h, respectively, whereas Fair-GPTQ completes quan-

tization in under 15 min (see §D). The quantized OPT-6.7B model is smaller and achieves faster inference; however, consistent with prior work on quantization, this acceleration comes at the cost of some degradation in downstream performance, explaining the trade-off reported in Table 3.

6 Conclusion

In this paper, we introduce FAIR-GPTQ, a fairness-aware quantization method with a bias-aware term that minimizes disparity between stereotypical and anti-stereotypical sentences. Unlike Optimal Brain Surgeon (Hassibi et al., 1993) and subsequent work on compression, our approach accounts for non-zero gradients during the quantization process. The implemented solution has the same computational complexity as GPTQ and can be applied to models of any size.

Next, we validate the method experimentally on models with different architectures and observe a reduced likelihood of stereotyped generations for models quantized with FAIR-GPTQ. When applying FAIR-GPTQ to a subset of layers, we find that targeting lower layers yields smaller social bias scores on stereotype benchmarks.

To the best of our knowledge, this work is the first to study biases in quantization, providing insights into how weights from different matrix types and layers might contribute to group bias. Building on this foundation, future work may leverage gradient information to guide quantization, adapt the method for outlier detection (Dettmers et al., 2022a), or explore the use of half-precision outlier channels (Lee et al., 2024) to recover the performance of debiased models.

References

- Yonatan Bisk, Rowan Zellers, Jianfeng Gao, Yejin Choi, et al. 2020. [PiQA: Reasoning about physical commonsense in natural language](#). In *Proceedings of the AAAI conference on artificial intelligence*, volume 34, pages 7432–7439.
- Tolga Bolukbasi, Kai-Wei Chang, James Y Zou, Venkatesh Saligrama, and Adam T Kalai. 2016. Man is to computer programmer as woman is to homemaker? debiasing word embeddings. *Advances in neural information processing systems*, 29.
- Shikha Bordia and Samuel R. Bowman. 2019. [Identifying and reducing gender bias in word-level language models](#). In *Proceedings of the 2019 Conference of the North American Chapter of the Association for Computational Linguistics: Student Research Workshop*, pages 7–15, Minneapolis, Minnesota. Association for Computational Linguistics.
- Tom Brown, Benjamin Mann, Nick Ryder, Melanie Subbiah, Jared D Kaplan, Prafulla Dhariwal, Arvind Neelakantan, Pranav Shyam, Girish Sastry, Amanda Askell, et al. 2020. Language models are few-shot learners. *Advances in neural information processing systems*, 33:1877–1901.
- Aylin Caliskan, Joanna J Bryson, and Arvind Narayanan. 2017. Semantics derived automatically from language corpora contain human-like biases. *Science*, 356(6334):183–186.
- Jerry Chee, Yaohui Cai, Volodymyr Kuleshov, and Christopher M De Sa. 2023. Quip: 2-bit quantization of large language models with guarantees. *Advances in Neural Information Processing Systems*, 36:4396–4429.
- Peter Clark, Isaac Cowhey, Oren Etzioni, Tushar Khot, Ashish Sabharwal, Carissa Schoenick, and Oyvind Tafjord. 2018. [Think you have solved question answering? Try ARC, the AI2 reasoning challenge](#). *CoRR*, abs/1803.05457.
- Thomas Davidson, Debasmita Bhattacharya, and Ingmar Weber. 2019. [Racial bias in hate speech and abusive language detection datasets](#). In *Proceedings of the Third Workshop on Abusive Language Online*, pages 25–35, Florence, Italy. Association for Computational Linguistics.
- Tim Dettmers, Mike Lewis, Younes Belkada, and Luke Zettlemoyer. 2022a. [Gpt3.int8\(\): 8-bit matrix multiplication for transformers at scale](#). *Advances in neural information processing systems*, 35:30318–30332.
- Tim Dettmers, Mike Lewis, Younes Belkada, and Luke Zettlemoyer. 2022b. [Gpt3.int8\(\): 8-bit matrix multiplication for transformers at scale](#). In *Advances in Neural Information Processing Systems*, volume 35, pages 30318–30332. Curran Associates, Inc.
- Nelson Elhage, Neel Nanda, Catherine Olsson, Tom Henighan, Nicholas Joseph, Ben Mann, Amanda Askell, Yuntao Bai, Anna Chen, Tom Conerly, Nova DasSarma, Dawn Drain, Deep Ganguli, Zac Hatfield-Dodds, Danny Hernandez, Andy Jones, Jackson Kernion, Liane Lovitt, Kamal Ndousse, Dario Amodei, Tom Brown, Jack Clark, Jared Kaplan, Sam McCandlish, and Chris Olah. 2021. A mathematical framework for transformer circuits. *Transformer Circuits Thread*. <https://transformer-circuits.pub/2021/framework/index.html>.
- Shangbin Feng, Chan Young Park, Yuhan Liu, and Yulia Tsvetkov. 2023. [From pretraining data to language models to downstream tasks: Tracking the trails of political biases leading to unfair NLP models](#). In *Proceedings of the 61st Annual Meeting of the Association for Computational Linguistics (Volume 1: Long Papers)*, pages 11737–11762, Toronto, Canada. Association for Computational Linguistics.
- Elias Frantar and Dan Alistarh. 2022. Optimal brain compression: A framework for accurate post-training quantization and pruning. *Advances in Neural Information Processing Systems*, 35:4475–4488.
- Elias Frantar, Saleh Ashkboos, Torsten Hoefler, and Dan Alistarh. 2022. Gptq: Accurate post-training quantization for generative pre-trained transformers. *arXiv preprint arXiv:2210.17323*.
- Elias Frantar, Roberto L Castro, Jiale Chen, Torsten Hoefler, and Dan Alistarh. 2025. Marlin: Mixed-precision auto-regressive parallel inference on large language models. In *Proceedings of the 30th ACM SIGPLAN Annual Sym-*

- posium on Principles and Practice of Parallel Programming*, pages 239–251.
- Mor Geva, Roei Schuster, Jonathan Berant, and Omer Levy. 2021. [Transformer feed-forward layers are key-value memories](#). In *Proceedings of the 2021 Conference on Empirical Methods in Natural Language Processing*, pages 5484–5495, Online and Punta Cana, Dominican Republic. Association for Computational Linguistics.
- Gustavo Gonçalves and Emma Strubell. 2023. [Understanding the effect of model compression on social bias in large language models](#). In *Proceedings of the 2023 Conference on Empirical Methods in Natural Language Processing*, pages 2663–2675, Singapore. Association for Computational Linguistics.
- Aaron Grattafiori, Abhimanyu Dubey, Abhinav Jauhri, Abhinav Pandey, Abhishek Kadian, Ahmad Al-Dahle, Aiesha Letman, Akhil Mathur, Alan Schelten, Alex Vaughan, et al. 2024. The llama 3 herd of models. *arXiv preprint arXiv:2407.21783*.
- Sylvain Gugger, Lysandre Debut, Thomas Wolf, Philipp Schmid, Zachary Mueller, Sourab Mangrulkar, Marc Sun, and Benjamin Bossan. 2022. Accelerate: Training and inference at scale made simple, efficient and adaptable. <https://github.com/huggingface/accelerate>.
- Babak Hassibi, David G Stork, and Gregory J Wolff. 1993. Optimal brain surgeon and general network pruning. In *IEEE international conference on neural networks*, pages 293–299. IEEE.
- Jung Hwan Heo, Jeonghoon Kim, Beomseok Kwon, Byeongwook Kim, Se Jung Kwon, and Dongsoo Lee. 2023. Rethinking channel dimensions to isolate outliers for low-bit weight quantization of large language models. *arXiv preprint arXiv:2309.15531*.
- Itay Hubara, Yury Nahshan, Yair Hanani, Ron Banner, and Daniel Soudry. 2021. Accurate post training quantization with small calibration sets. In *International conference on machine learning*, pages 4466–4475. PMLR.
- Ajay Jaiswal, Zhe Gan, Xianzhi Du, Bowen Zhang, Zhangyang Wang, and Yinfei Yang. 2023. Compressing llms: The truth is rarely pure and never simple. *arXiv preprint arXiv:2310.01382*.
- Fred Jelinek, Robert L Mercer, Lalit R Bahl, and James K Baker. 1977. Perplexity—a measure of the difficulty of speech recognition tasks. *The Journal of the Acoustical Society of America*, 62(S1):S63–S63.
- Albert Q. Jiang, Alexandre Sablayrolles, Arthur Mensch, Chris Bamford, Devendra Singh Chaplot, Diego de las Casas, Florian Bressand, Gianna Lengyel, Guillaume Lample, Lucile Saulnier, Léo Renard Lavaud, Marie-Anne Lachaux, Pierre Stock, Teven Le Scao, Thibaut Lavril, Thomas Wang, Timothée Lacroix, and William El Sayed. 2023. [Mistral 7b](#).
- Jared Kaplan, Sam McCandlish, Tom Henighan, Tom B. Brown, Benjamin Chess, Rewon Child, Scott Gray, Alec Radford, Jeff Wu, and Dario Amodei. 2020. [Scaling laws for neural language models](#). *ArXiv*, abs/2001.08361.
- Yann LeCun, John Denker, and Sara Solla. 1989. Optimal brain damage. *Advances in neural information processing systems*, 2.
- Changhun Lee, Jungyu Jin, Taesu Kim, Hyungjun Kim, and Eunhyeok Park. 2024. Owq: Outlier-aware weight quantization for efficient fine-tuning and inference of large language models. In *Proceedings of the AAAI Conference on Artificial Intelligence*, volume 38, pages 13355–13364.
- Tao Li, Daniel Khashabi, Tushar Khot, Ashish Sabharwal, and Vivek Srikumar. 2020. [UNQOVERing stereotyping biases via underspecified questions](#). In *Findings of the Association for Computational Linguistics: EMNLP 2020*, pages 3475–3489, Online. Association for Computational Linguistics.
- Paul Pu Liang, Irene Mengze Li, Emily Zheng, Yao Chong Lim, Ruslan Salakhutdinov, and Louis-Philippe Morency. 2020. [Towards debiasing sentence representations](#). In *Proceedings of the 58th Annual Meeting of the Association for Computational Linguistics*, pages 5502–5515, Online. Association for Computational Linguistics.

- Ji Lin, Jiaming Tang, Haotian Tang, Shang Yang, Wei-Ming Chen, Wei-Chen Wang, Guangxuan Xiao, Xingyu Dang, Chuang Gan, and Song Han. 2024. Awq: Activation-aware weight quantization for on-device llm compression and acceleration. *Proceedings of machine learning and systems*, 6:87–100.
- Peiyu Liu, Zikang Liu, Ze-Feng Gao, Dawei Gao, Wayne Xin Zhao, Yaliang Li, Bolin Ding, and Ji rong Wen. 2023. Do emergent abilities exist in quantized large language models: An empirical study. *ArXiv*, abs/2307.08072.
- Thomas Manzini, Lim Yao Chong, Alan W Black, and Yulia Tsvetkov. 2019. Black is to criminal as Caucasian is to police: Detecting and removing multiclass bias in word embeddings. In *Proceedings of the 2019 Conference of the North American Chapter of the Association for Computational Linguistics: Human Language Technologies, Volume 1 (Long and Short Papers)*, pages 615–621, Minneapolis, Minnesota. Association for Computational Linguistics.
- Kelly Marchisio, Saurabh Dash, Hongyu Chen, Dennis Aumiller, Ahmet Üstün, Sara Hooker, and Sebastian Ruder. 2024. How does quantization affect multilingual LLMs? In *Findings of the Association for Computational Linguistics: EMNLP 2024*, pages 15928–15947, Miami, Florida, USA. Association for Computational Linguistics.
- Nicholas Meade, Elinor Poole-Dayana, and Siva Reddy. 2022. An empirical survey of the effectiveness of debiasing techniques for pre-trained language models. In *Proceedings of the 60th Annual Meeting of the Association for Computational Linguistics (Volume 1: Long Papers)*, pages 1878–1898, Dublin, Ireland. Association for Computational Linguistics.
- Stephen Merity, Caiming Xiong, James Bradbury, and Richard Socher. 2016. Pointer sentinel mixture models. *arXiv preprint arXiv:1609.07843*.
- Alireza Mohammadshahi, Vassilina Nikoulina, Alexandre Berard, Caroline Brun, James Henderson, and Laurent Besacier. 2022. What do compressed multilingual machine translation models forget? In *Findings of the Association for Computational Linguistics: EMNLP 2022*, pages 4308–4329, Abu Dhabi, United Arab Emirates. Association for Computational Linguistics.
- Nasrin Mostafazadeh, Michael Roth, Annie Louis, Nathanael Chambers, and James Allen. 2017. LSDSem 2017 shared task: The story cloze test. In *Proceedings of the 2nd Workshop on Linking Models of Lexical, Sentential and Discourse-level Semantics*, pages 46–51, Valencia, Spain. Association for Computational Linguistics.
- Moin Nadeem, Anna Bethke, and Siva Reddy. 2021. StereoSet: Measuring stereotypical bias in pretrained language models. In *Proceedings of the 59th Annual Meeting of the Association for Computational Linguistics and the 11th International Joint Conference on Natural Language Processing (Volume 1: Long Papers)*, pages 5356–5371, Online. Association for Computational Linguistics.
- Markus Nagel, Rana Ali Amjad, Mart Van Baalen, Christos Louizos, and Tijmen Blankevoort. 2020. Up or down? adaptive rounding for post-training quantization. In *International conference on machine learning*, pages 7197–7206. PMLR.
- Nikita Nangia, Clara Vania, Rasika Bhalerao, and Samuel R. Bowman. 2020. CrowS-pairs: A challenge dataset for measuring social biases in masked language models. In *Proceedings of the 2020 Conference on Empirical Methods in Natural Language Processing (EMNLP)*, pages 1953–1967, Online. Association for Computational Linguistics.
- Ali Omrani, Alireza Salkhordeh Ziabari, Charles Yu, Prenti Golazizian, Brendan Kennedy, Mohammad Atari, Heng Ji, and Morteza Dehghani. 2023. Social-group-agnostic bias mitigation via the stereotype content model. In *Proceedings of the 61st Annual Meeting of the Association for Computational Linguistics (Volume 1: Long Papers)*, pages 4123–4139, Toronto, Canada. Association for Computational Linguistics.
- Alicia Parrish, Angelica Chen, Nikita Nangia, Vishakh Padmakumar, Jason Phang, Jana Thompson, Phu Mon Htut, and Samuel Bowman. 2022. BBQ: A hand-built bias benchmark for question answering. In *Findings of the Association for Computational Linguistics: ACL*

- 2022, pages 2086–2105, Dublin, Ireland. Association for Computational Linguistics.
- Adam Paszke, Sam Gross, Francisco Massa, Adam Lerer, James Bradbury, Gregory Chanan, Trevor Killeen, Zeming Lin, Natalia Gimelshein, Luca Antiga, et al. 2019. Pytorch: An imperative style, high-performance deep learning library. *Advances in neural information processing systems*, 32.
- Nirmalendu Prakash and Roy Ka-Wei Lee. 2023. [Layered bias: Interpreting bias in pretrained large language models](#). In *Proceedings of the 6th BlackboxNLP Workshop: Analyzing and Interpreting Neural Networks for NLP*, pages 284–295, Singapore. Association for Computational Linguistics.
- Colin Raffel, Noam M. Shazeer, Adam Roberts, Katherine Lee, Sharan Narang, Michael Matena, Yanqi Zhou, Wei Li, and Peter J. Liu. 2019. [Exploring the limits of transfer learning with a unified text-to-text transformer](#). *J. Mach. Learn. Res.*, 21:140:1–140:67.
- Krithika Ramesh, Arnav Chavan, Shrey Pandit, and Sunayana Sitaram. 2023. [A comparative study on the impact of model compression techniques on fairness in language models](#). In *Proceedings of the 61st Annual Meeting of the Association for Computational Linguistics (Volume 1: Long Papers)*, pages 15762–15782, Toronto, Canada. Association for Computational Linguistics.
- Shauli Ravfogel, Yanai Elazar, Hila Gonen, Michael Twiton, and Yoav Goldberg. 2020. [Null it out: Guarding protected attributes by iterative nullspace projection](#). In *Proceedings of the 58th Annual Meeting of the Association for Computational Linguistics*, pages 7237–7256, Online. Association for Computational Linguistics.
- Timo Schick, Sahana Udupa, and Hinrich Schütze. 2021. [Self-diagnosis and self-debiasing: A proposal for reducing corpus-based bias in NLP](#). *Transactions of the Association for Computational Linguistics*, 9:1408–1424.
- Ryan Steed, Swetasudha Panda, Ari Kobren, and Michael Wick. 2022. Upstream mitigation is not all you need: Testing the bias transfer hypothesis in pre-trained language models. In *Proceedings of the 60th Annual Meeting of the Association for Computational Linguistics (Volume 1: Long Papers)*, pages 3524–3542.
- Thomas Wolf, Lysandre Debut, Victor Sanh, Julien Chaumond, Clement Delangue, Anthony Moi, Pierric Cistac, Tim Rault, Remi Louf, Morgan Funtowicz, et al. 2020. Transformers: State-of-the-art natural language processing. In *Proceedings of the 2020 conference on empirical methods in natural language processing: system demonstrations*, pages 38–45.
- Guangxuan Xiao, Ji Lin, Mickael Seznec, Hao Wu, Julien Demouth, and Song Han. 2023. Smoothquant: Accurate and efficient post-training quantization for large language models. In *International conference on machine learning*, pages 38087–38099. PMLR.
- Zhichao Xu, Ashim Gupta, Tao Li, Oliver Bentham, and Vivek Srikumar. 2024. [Beyond perplexity: Multi-dimensional safety evaluation of LLM compression](#). In *Findings of the Association for Computational Linguistics: EMNLP 2024*, pages 15359–15396, Miami, Florida, USA. Association for Computational Linguistics.
- Zhewei Yao, Reza Yazdani Aminabadi, Minjia Zhang, Xiaoxia Wu, Conglong Li, and Yuxiong He. 2022. Zeroquant: Efficient and affordable post-training quantization for large-scale transformers. *Advances in Neural Information Processing Systems*, 35:27168–27183.
- Rowan Zellers, Ari Holtzman, Yonatan Bisk, Ali Farhadi, and Yejin Choi. 2019. [HellaSwag: Can a machine really finish your sentence?](#) In *Proceedings of the 57th Annual Meeting of the Association for Computational Linguistics*, pages 4791–4800, Florence, Italy. Association for Computational Linguistics.
- Susan Zhang, Stephen Roller, Naman Goyal, Mikel Artetxe, Moya Chen, Shuohui Chen, Christopher Dewan, Mona Diab, Xian Li, Xi Victoria Lin, et al. 2022. Opt: Open pre-trained transformer language models. *arXiv preprint arXiv:2205.01068*.
- Hanzhang Zhou, Zijian Feng, Zixiao Zhu, Junlang Qian, and Kezhi Mao. 2024. Unibias:

Unveiling and mitigating llm bias through internal attention and ffn manipulation. *Advances in Neural Information Processing Systems*, 37:102173–102196.

Xunyu Zhu, Jian Li, Yong Liu, Can Ma, and Weiping Wang. 2024. A survey on model compression for large language models. *Transactions of the Association for Computational Linguistics*, 12:1556–1577.

Ran Zmigrod, Sabrina J. Mielke, Hanna Wallach, and Ryan Cotterell. 2019. [Counterfactual data augmentation for mitigating gender stereotypes in languages with rich morphology](#). In *Proceedings of the 57th Annual Meeting of the Association for Computational Linguistics*, pages 1651–1661, Florence, Italy. Association for Computational Linguistics.

A Proof of Proposition 1

We recall that the aim is to solve the Problem (2) column by column. Before providing the proof of Proposition 1, we first restate the Optimization Problem (6) where the aim is to find the optimal modification $\Delta \mathbf{w}$ to apply to the flattened version \mathbf{w} of \mathbf{W} , such that:

$$\begin{aligned} \min_{\Delta \mathbf{w}} \quad & \mathbf{J}_{\mathbf{w}}^{\top} \Delta \mathbf{w} + \frac{1}{2} \Delta \mathbf{w}^{\top} \mathbf{H}_{\mathbf{w}} \Delta \mathbf{w}, \\ \text{s.t.} \quad & \mathbf{e}_q^{\top} \Delta \mathbf{w} = \text{quant}(w_q) - w_q, \end{aligned}$$

where $\mathbf{J}_{\mathbf{w}}$ and $\mathbf{H}_{\mathbf{w}}$ are the first and second order derivative respectively of the flattened version of the objective function defined in Eq. (2).

Proposition 2 (Weight updates and their impact). *Let us consider the optimization problem defined by Eq. (6) The optimal weight modification $\Delta \mathbf{w}^*$ to apply to \mathbf{w} is given by:*

$$\Delta \mathbf{w}^* = -\mathbf{H}_{\mathbf{w}}^{-1} \mathbf{J}_{\mathbf{w}} - \frac{w_q - \text{quant}(w_q) - \mathbf{e}_q^{\top} \mathbf{H}_{\mathbf{w}}^{-1} \mathbf{J}_{\mathbf{w}}}{[\mathbf{H}_{\mathbf{w}}^{-1}]_{qq}} \mathbf{H}_{\mathbf{w}}^{-1} \mathbf{e}_q. \quad (9)$$

and the saliency associated to the modification is given by:

$$\Delta f = \frac{(w_q - \text{quant}(w_q) - \mathbf{e}_q^{\top} \mathbf{H}_{\mathbf{w}}^{-1} \mathbf{J}_{\mathbf{w}})^2}{2[\mathbf{H}_{\mathbf{w}}^{-1}]_{qq}} - \frac{1}{2} \mathbf{J}_{\mathbf{w}}^{\top} \mathbf{H}_{\mathbf{w}}^{-1} \mathbf{J}_{\mathbf{w}}. \quad (10)$$

Proof. We start from the Lagrangian of the optimization problem:

$$L(\Delta \mathbf{w}, \lambda) = \mathbf{J}_{\mathbf{w}}^{\top} \Delta \mathbf{w} + \frac{1}{2} \Delta \mathbf{w}^{\top} \mathbf{H}_{\mathbf{w}} \Delta \mathbf{w} + \lambda \left(\mathbf{e}_q^{\top} \Delta \mathbf{w} + w_q - \text{quant}(w_q) \right)$$

We will first express the change of the weights with respect to λ , *i.e.*, the Lagrange multiplier using its first order derivative *w.r.t.* to $\Delta \mathbf{w}$. More formally, we will compute $\frac{\partial L}{\partial \Delta \mathbf{w}}(\Delta \mathbf{w}, \lambda)$ and study which change in $\Delta \mathbf{w}$ leads to the minimum value of the Lagrangian.

$$\begin{aligned} \frac{\partial L}{\partial \Delta \mathbf{w}}(\Delta \mathbf{w}, \lambda) = \mathbf{0} & \iff \mathbf{H}_{\mathbf{w}} \Delta \mathbf{w} + \mathbf{J}_{\mathbf{w}} + \lambda \mathbf{e}_q = \mathbf{0}, \\ & \iff \Delta \mathbf{w} = -\mathbf{H}_{\mathbf{w}}^{-1} (\lambda \mathbf{e}_q + \mathbf{J}_{\mathbf{w}}). \end{aligned}$$

We can now express the Lagrangian with respect to λ only.

$$\begin{aligned} L(\lambda) &= \frac{1}{2} \left(\mathbf{H}_{\mathbf{w}}^{-1} (\lambda \mathbf{e}_q + \mathbf{J}_{\mathbf{w}}) \right)^{\top} \mathbf{H}_{\mathbf{w}} \left(\mathbf{H}_{\mathbf{w}}^{-1} (\lambda \mathbf{e}_q + \mathbf{J}_{\mathbf{w}}) \right) - \mathbf{J}_{\mathbf{w}}^{\top} \left(\mathbf{H}_{\mathbf{w}}^{-1} (\lambda \mathbf{e}_q + \mathbf{J}_{\mathbf{w}}) \right) \\ &\quad + \lambda \left[-\mathbf{e}_q^{\top} \mathbf{H}_{\mathbf{w}}^{-1} (\lambda \mathbf{e}_q + \mathbf{J}_{\mathbf{w}}) + w_q - \text{quant}(w_q) \right], \\ &= \frac{1}{2} (\lambda \mathbf{e}_q + \mathbf{J}_{\mathbf{w}})^{\top} \mathbf{H}_{\mathbf{w}}^{-1} (\lambda \mathbf{e}_q + \mathbf{J}_{\mathbf{w}}) - \lambda \mathbf{J}_{\mathbf{w}}^{\top} \mathbf{H}_{\mathbf{w}}^{-1} \mathbf{e}_q - \mathbf{J}_{\mathbf{w}}^{\top} \mathbf{H}_{\mathbf{w}}^{-1} \mathbf{J}_{\mathbf{w}} - \lambda^2 \mathbf{e}_q^{\top} \mathbf{H}_{\mathbf{w}}^{-1} \mathbf{e}_q \\ &\quad + \lambda \left[-\mathbf{e}_q^{\top} \mathbf{H}_{\mathbf{w}}^{-1} \mathbf{J}_{\mathbf{w}} + w_q - \text{quant}(w_q) \right], \\ &= \frac{\lambda^2}{2} \mathbf{e}_q^{\top} \mathbf{H}_{\mathbf{w}}^{-1} \mathbf{e}_q + \frac{1}{2} \mathbf{J}_{\mathbf{w}}^{\top} \mathbf{H}_{\mathbf{w}}^{-1} \mathbf{J}_{\mathbf{w}} - \mathbf{J}_{\mathbf{w}}^{\top} \mathbf{H}_{\mathbf{w}}^{-1} \mathbf{J}_{\mathbf{w}} + \underbrace{\lambda \mathbf{J}_{\mathbf{w}}^{\top} \mathbf{H}_{\mathbf{w}}^{-1} \mathbf{e}_q - \lambda \mathbf{J}_{\mathbf{w}}^{\top} \mathbf{H}_{\mathbf{w}}^{-1} \mathbf{e}_q}_{=0} \\ &\quad - \lambda^2 \mathbf{e}_q^{\top} \mathbf{H}_{\mathbf{w}}^{-1} \mathbf{e}_q + \lambda \left[-\mathbf{e}_q^{\top} \mathbf{H}_{\mathbf{w}}^{-1} \mathbf{J}_{\mathbf{w}} + w_q - \text{quant}(w_q) \right], \\ &= -\frac{\lambda^2}{2} \mathbf{e}_q^{\top} \mathbf{H}_{\mathbf{w}}^{-1} \mathbf{e}_q - \lambda (\mathbf{e}_q^{\top} \mathbf{H}_{\mathbf{w}}^{-1} \mathbf{J}_{\mathbf{w}} - (w_q - \text{quant}(w_q))) - \frac{1}{2} \mathbf{J}_{\mathbf{w}}^{\top} \mathbf{H}_{\mathbf{w}}^{-1} \mathbf{J}_{\mathbf{w}}. \end{aligned}$$

We can now rewrite the Lagrangian can be rewritten as

$$L(\lambda) = -\frac{\lambda^2}{2}[\mathbf{H}_w^{-1}]_{qq} - \lambda(\mathbf{e}_q^\top \mathbf{H}_w^{-1} \mathbf{J}_w - (w_q - \text{quant}(w_q))) - \frac{1}{2} \mathbf{J}_w^\top \mathbf{H}_w^{-1} \mathbf{J}_w,$$

where $[\mathbf{H}_w]_{qq}$ designates the q -th element on the diagonal of the \mathbf{H}_w matrix.

We compute the derivative of the Lagrangian in order to find the optimal value λ for which the Lagrangian reaches its maximum.

$$\begin{aligned} \frac{\partial L}{\partial \lambda}(\lambda) = 0 &\iff -\lambda[\mathbf{H}_w^{-1}]_{qq} + w_q - \text{quant}(w_q) - \mathbf{e}_q^\top \mathbf{H}_w^{-1} \mathbf{J}_w = 0, \\ &\iff \lambda = \frac{w_q - \text{quant}(w_q) - \mathbf{e}_q^\top \mathbf{H}_w^{-1} \mathbf{J}_w}{[\mathbf{H}_w^{-1}]_{qq}}. \end{aligned}$$

Furthermore, we also know that

$$\mathbf{H}_w \Delta \mathbf{w} + \mathbf{J}_w + \lambda \mathbf{e}_q = \mathbf{0} \iff \Delta \mathbf{w} = -\mathbf{H}_w^{-1}(\mathbf{J}_w + \lambda \mathbf{e}_q).$$

We finally have:

$$\Delta \mathbf{w} = -\mathbf{H}_w^{-1} \mathbf{J}_w - \frac{w_q - \text{quant}(w_q) - \mathbf{e}_q^\top \mathbf{H}_w^{-1} \mathbf{J}_w}{[\mathbf{H}_w^{-1}]_{qq}} \mathbf{H}_w^{-1} \mathbf{e}_q. \quad (11)$$

It remains to study the change in loss occurred when we update w_q with the expression (9) of $\Delta \mathbf{w}$. This change is equal to:

$$L_q = -\frac{\lambda^2}{2}[\mathbf{H}_w^{-1}]_{qq} - \lambda(\mathbf{e}_q^\top \mathbf{H}_w^{-1} \mathbf{J}_w - (w_q - \text{quant}(w_q))) - \frac{1}{2} \mathbf{J}_w^\top \mathbf{H}_w^{-1} \mathbf{J}_w,$$

where $\lambda = \frac{w_q - \text{quant}(w_q) - \mathbf{e}_q^\top \mathbf{H}_w^{-1} \mathbf{J}_w}{[\mathbf{H}_w^{-1}]_{qq}}$.

This last expression can be simplified as follows:

$$L_q = \frac{(w_q - \text{quant}(w_q) - \mathbf{e}_q^\top \mathbf{H}_w^{-1} \mathbf{J}_w)^2}{2[\mathbf{H}_w^{-1}]_{qq}} - \frac{1}{2} \mathbf{J}_w^\top \mathbf{H}_w^{-1} \mathbf{J}_w = \Delta f. \quad (12)$$

□

B Benchmark Details

In this appendix, we provide a summary of the benchmarks used for evaluation. For all the benchmarks, we utilize the official implementation unless explicitly stated otherwise. To assess perplexity, we employ the implementation provided by the Transformers' Evaluate library⁸, based on the standard perplexity metric proposed in (Jelinek et al., 1977).

B.1 Zero-Shot Benchmarks

For zero-shot benchmarks, we rely on the implementations provided by the LM Evaluation Harness framework.⁹ The reported accuracy metrics specifically refer to accuracy computed based on the likelihood of the model's generated answers. Additionally, we include random baselines for comparison in Table 4.

B.2 Fairness benchmarks

In this appendix, we provide details on the benchmarks used to evaluate the likelihood of stereotype generations.

⁸<https://huggingface.co/spaces/evaluate-metric/perplexity>

⁹<https://github.com/EleutherAI/lm-evaluation-harness>

Task	Type	Size	Avg. Input Length	Random Baseline
ARC-easy	Natural Language Inference	2376	113.60	25.0
HellaSwag	Sentence Completion	10003	219.30	25.0
PiQA	Multiple-choice Question Answering	21035	53.77	50.0
XStoryCloze	Sentence Completion	1511	185.60	50.0

Table 4: Overview of zero-shot and few-shot benchmarks.

Simple Co-occurrence (COOC) bias tests (Brown et al., 2020) focus on gender occupation bias and cover 388 occupations of the following type "*The {occupation} is*". The metric used to estimate the bias measures the average log-probability ratio of female to male terms following occupational prompts under different contextual framings:

$$\frac{1}{n_{\text{jobs}}} \sum_{\text{jobs}} \log \left(\frac{P(\text{female}|\text{context})}{P(\text{male}|\text{context})} \right).$$

CrowS-Pairs (Nangia et al., 2020) is crowd-sourced dataset of minimal pairs that covers nine axes - gender, race, sexual orientation, religion, age, nationality, disability, physical appearance and occupation. Bias is quantified as the percentage of pairs for which the model assigns higher likelihood to the stereotyped sentence than to its anti-stereotyped counterpart. We use implementation for generative models from Gonçalves and Strubell (2023) for bias measurement.

StereoSet (Nadeem et al., 2021) is a crowd-sourced dataset of triplet sentences, each consisting of a stereotype, anti-stereotype, and an unrelated (meaningless) sentence. StereoSet covers four demographical axes: gender, race, religion, and profession. The bias score is the percentage of examples in which a model prefers a stereotypical association over an anti-stereotypical association. The language modeling score (LMS) is the percentage of instances in which a language model prefers the meaningful (stereotyped or anti-stereotyped) over the meaningless association.

BBQ (Parrish et al., 2022) is a question-answering dataset created to measure how social biases influence model answer generation, specifically when such biases alter the model’s predictions. The question templates, written by the authors, cover nine protected categories (sexual orientation, religion, race/ethnicity, physical appearance, nationality, gender, gender identity, socio-economic status, and disability status) along with two intersectional categories: gender by race/ethnicity and socio-economic status by race/ethnicity. These templates draw on documented stereotypes from research studies, news reports, Wikipedia, and personal accounts. The dataset contains two types of questions: ambiguous and disambiguated. Validation was conducted with human annotators, achieving high agreement scores. Given a question, the model must choose which of two individuals engaged in a possibly stereotypical behavior (e.g., *Who showed forgetfulness: a 40-year-old or a 20-year-old?*). In ambiguous contexts, the correct answer is UNKNOWN, and accuracy reflects how often the model selects this option instead of the stereotypical choice. In disambiguated contexts, where contextual cues indicate the anti-stereotypical answer, accuracy measures whether the model follows the evidence rather than the stereotype. Bias in both cases is quantified as the frequency with which the model selects the stereotypical option. Bias score in disambiguated contexts is calculated as: $s_{\text{DIS}} = 2 \cdot \left(\frac{n_{\text{biased_ans}}}{n_{\text{non-UNKNOWN_outputs}}} \right) - 1$. Bias score in ambiguous contexts is computed given the bias score in disambiguated contexts: $s_{\text{AMB}} = (1 - \text{accuracy}) \cdot s_{\text{DIS}}$

UnQover (Li et al., 2020) is a large dataset consisting of ambiguous question-answer pairs spanning the demographic axes of gender, nationality, ethnicity, and religion. The correct answer is always *Unknown* or *Not Determined*. We sample 10k examples from each QA category and evaluate accuracy, defined as the number of times the model selects the correct answer.

We rely on the implementations provided by the LM EVALUATION HARNESS framework. For STEREOSET and UNQOVER, we use the original metric implementations released by the respective authors.

C Debiasing baselines

We briefly present the methodology of our three competitors.

Benchmark	Axes	N Sent. (Dev./Test)
BBQ (Parrish et al., 2022)	11	-/58,492
CrowS-Pairs (Nangia et al., 2020)	9	-/3016
StereoSet (Nadeem et al., 2021)	4	2106/6392
UnQover (Li et al., 2020)	4	-/40,000

Table 5: Overview of benchmarks for stereotype skew measurements

INLP (Ravfogel et al., 2020) The idea is to learn a new representation of the data \mathbf{x} using their encoded representation $\text{enc}(\mathbf{x})$ which is independent from the sensitive attributes \mathbf{z} . More precisely, they learn a projection \mathbf{P} such that there is no more linear relation between the sensitive attribute and the projected data $\mathbf{P}(\text{enc}(\mathbf{x}))$, *i.e.*, $\mathbf{W}\mathbf{P}(\text{enc}(\mathbf{x})) = \mathbf{0}, \forall \mathbf{W}$. If such a constrained is satisfied then the learned model is said to be *fair*.

In practice, they learn a first model f , *e.g.* a neural network, which aims to predict the target label using the encoded representation of \mathbf{x} . Then they fine tune their model using, namely the last layer of the network, by applying INLP to the encoded representation $\text{enc}(\mathbf{x})$ and update the last layer weights.

Self-Debias (Schick et al., 2021) First, the language model is constrained to generate a toxic, potentially offensive text on sensitive information, such as gender, religion, *etc.* The model is then asked to perform a self-diagnosis using this toxic text. A probability is computed between the initial text and its emphasized toxic version and used to reduce the probability of tokens involved in the toxic text generation.

SentenceDebias We use method introduced by Liang et al. (2020) which works on the words representation. More formally, they aim to learn an unbiased representation. To do so, they first define a subspace, called *biased* one, defined by all the words that may reflect bias (*e.g.* *he/she* for gender). Then, all the representations are projected onto the subspace orthogonal to *biased* one.

We use the debiasing baseline implementations from the BIASBENCH framework by Meade et al. (2022) and integrate generative model support into the framework.

D Runtime Comparison

We measure the quantization time of models using Fair-GPTQ ALL and GPTQ-SS. Results for the largest models are reported in Table 6. We find that quantization runtime increases by around 2 minutes.

Model	GPTQ-SS	Fair-GPTQ <small>ALL</small>
OPT-6.7B	7.98m	10.40m
OPT-13B	16.69m	17.10m
Mistral-7B	8.07m	10.59m

Table 6: Comparison of the overall runtime of GPTQ-SS and Fair-GPTQ_{ALL} in minutes.

E Sanity-Check Experiments

We evaluate the performance of models quantized using unrelated pairs from STEREOSET. The goal of this study is twofold: (1) to assess the usefulness of the STEREOSET dataset as calibration data \mathbf{X} for quantization, and (2) to determine whether reductions in stereotype scores arise from genuine debiasing rather than from performance degradation. To generate the unrelated pairs, we use the Mistral-Instruct-8B model. We prompt it with the following instruction:

“You are a helpful assistant that generates syntactically valid but semantically nonsensical sentences based on a given context sentence containing a BLANK token. Fill the BLANK with a grammatically correct word, but make the sentence unrelated or nonsensical. Do not leave the BLANK placeholder unchanged.” We use inter-sentence STEREOSET development set, which contains 2,106 context sentences

with a BLANK token. As a result, for example, given the context sentence: “The hispanic is usually BLANK.” the model produces unrelated alternatives such as: “The hispanic is usually tall.” “The hispanic is usually wise.” We quantize the OPT-1.3B model on paired unrelated data (\mathbf{X}_0 and \mathbf{X}_1). As a simple baseline, we also evaluate a setting where stereotypical and anti-stereotypical sentences are not paired correctly but instead mixed, such that the two come from different pairs. The results are reported in Table 7.

Strategy	PPL↓	ArcE↑	HSwag↑	CP _{pct} ↓
FP16	13.97	57.20	41.52	65.47
GPTQ-SS	15.50	56.19	40.75	65.47
GPTQ-random ALL	97.92	43.48	31.44	62.49
GPTQ-random L	15602.06	25.63	26.06	47.88
GPTQ-random U	353.10	35.98	32.52	58.02
GPTQ-random UL	10903.19	25.25	26.07	46.57
GPTQ-unrelated ALL	17.49	46.80	39.28	64.63
GPTQ-unrelated L	7956.45	25.97	25.84	48.66
GPTQ-unrelated U	23.89	48.61	38.25	64.55
GPTQ-unrelated UL	12456.16	25.42	26.23	49.49
Fair-GPTQ ALL	16.51	54.38	39.66	62.91
Fair-GPTQ L	17.43	54.29	40.10	59.57
Fair-GPTQ U	16.43	54.88	40.50	63.98
Fair-GPTQ UL	18.99	53.20	39.67	59.09

Table 7: Evaluation of OPT-1.3B quantized on pairs of unrelated sentences instead of stereotypical–anti-stereotypical data from STEREOSET (GPTQ-unrelated), and on mixed random pairs of stereotypical and anti-stereotypical sentences (GPTQ-random).

F Limitations and Future Work

While in this work we validate that the introduced method, FAIR-GPTQ, enables debiasing during quantization and scales across different model sizes for OPT, we acknowledge several limitations.

First, our calibration data (StereoSet) are limited to short sequences. Recent works have shown that calibration data impact generation quality for longer continuations. When estimating performance on zero-shot tasks, we find that the GPTQ-SS baseline scores are close to GPTQ-C4; however, we highlight that existing stereotype and non-stereotype dataset pairs are constrained to short passages of at most 2 to 3 sentences. To address this, in future work we plan to introduce an extended dataset that provides additional context, forming story-like narratives while preserving minimal differences for stereotypes. For example, instead of *He/She is a nurse*, a narrative may read *She always dreamt of becoming a nurse to help people. After graduation from college, she...*

Second, multilingual limitations remain. The calibration datasets we use are monolingual, whereas multilingual calibration data would be expected to improve performance for multilingual models.

Third, our experiments are restricted to a subset of model families. Although we report results for OPT and Mistral, newer models such as LLaMA-3 also be quantized with FAIR-GPTQ.

Finally, we do not experiment with multimodal models, which are increasingly prominent in NLP. Nonetheless, our approach could be extended to such models, as it is a modification of GPTQ, which can be used to quantize Transformer models in general.